



# Knoevenagel condensation reaction in zeolite membrane microreactor

Sau Man Lai <sup>a</sup>, Chi Po Ng <sup>a</sup>, Rosa Martin-Aranda <sup>b</sup>, King Lun Yeung <sup>a,\*</sup>

<sup>a</sup> Department of Chemical Engineering, The Hong Kong University of Science and Technology, Clear Water Bay, Kowloon, Hong Kong, SAR-PR China

<sup>b</sup> Departamento de Química Inorgánica y Química Técnica (UNED), Senda del Rey, 9, 28040, Madrid, Spain

Received 22 May 2003; received in revised form 18 September 2003; accepted 19 September 2003

## Abstract

The performance of a membrane microreactor was tested and compared with that of a microreactor, a packed bed reactor (PBR) and a packed bed membrane reactor (PBMR) for the Knoevenagel condensation reaction of benzaldehyde and ethyl cyanoacetate to produce ethyl 2-cyano-3-phenylacrylate. Cs-exchanged NaX faujasite zeolite was used as the base catalyst for this equilibrium-limited reaction. Hydrophilic ZSM-5 membranes were employed in both the membrane microreactor and the PBMR for the selective removal of water byproduct from the reaction. The product yield per pass was low for the packed bed reactor. Higher yields were observed for the microreactor and PBMR, but the best performance belongs to the membrane microreactor, which displayed both supra-equilibrium conversion and better product purity.

© 2003 Elsevier Inc. All rights reserved.

**Keywords:** ZSM-5 membrane; Cs-exchanged NaX; Microreactor; Membrane reactor; Supra-equilibrium conversion

## 1. Introduction

Fine chemicals and pharmaceuticals are high value added products that are produced in modest quantities. They are usually seasonal products that are customer specific and have a short shelf life. These characteristics usually place a significant constraint in their production, such that it is not uncommon to see labour intensive batch processes being used instead of the more efficient continuous

process. This usually leads to a significant waste generation during the scale-up from the laboratory to production scale. In addition, the use of hazardous and sometimes toxic homogeneous catalysts makes the product purification and waste disposal an important issue in today's stringent environmental regulations. Microchemical systems offer a new paradigm for meeting these challenges [1]. Recent advances in the design and fabrication of micromixers, microseparators and microreactors bring closer the realization of desktop miniature factories and micro-pharmacies [2–8]. They represent an alternative way for the production of specialty chemicals and pharmaceuticals by a *continuous* process, allowing simpler process

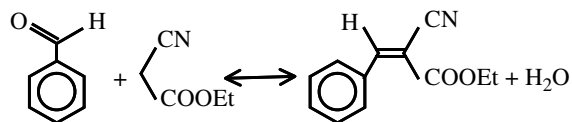
\* Corresponding author. Tel.: +852-2358-7123; fax: +852-2358-0054.

E-mail address: [kekyeung@ust.hk](mailto:kekyeung@ust.hk) (K.L. Yeung).

optimization, rapid design implementation, better safety and easier scale-up through replication. This enables rapid product deployment to the marketplace and thus ensuring a significant competitive edge.

Knoevenagel condensations of carbonylic compounds, activated methylene groups and malonic esters yield several important key products, such as the nitriles used in anionic polymerization and the  $\alpha$ ,  $\beta$ -unsaturated ester intermediates employed in the synthesis of several therapeutic drugs, e.g., nifendipine and nitrendipine. Unlike most condensation reactions, the Knoevenagel condensation is base-catalyzed. Homogeneous base catalysts such as pyridine and piperidine are traditionally used for these reactions [9]. Basic zeolites such as alkali cation exchanged *X* and *Y* zeolites [10–13], germanium-substituted faujasite [14] as well as cesium- and amino-modified mesoporous silicas [15,16] are also able to catalyze Knoevenagel condensation reactions. The use of a heterogeneous catalyst significantly simplifies product separation and purification. It also eliminates the need for solvents. However, the water formed by the reaction can poison the zeolite catalyst, and its removal is a must if we are to expect an optimum catalyst performance. The removal of water has the added benefit of increasing the conversion for this equilibrium limited reaction [17].

This study investigates the performance of a membrane microreactor for the Knoevenagel condensation of benzaldehyde and ethyl cyanoacetate to produce ethyl 2-cyano-3-phenylacrylate, a known intermediate for the preparation of fine chemicals.



The presence of the miniature membrane enables the continuous and selective removal of water during the reaction. Cesium-exchanged NaX faujasite was selected as the catalyst and ZSM-5

zeolite as the membrane. Several strategies for incorporating zeolite in microsystems have been described by Wan and coworkers [18,19]. Very precise and localized addition of zeolite materials was obtained and direct engineering of the deposited zeolite's microstructure and chemistry was also demonstrated. This enabled the successful integration of zeolite catalysts, films and membranes within the design architecture of microreactors and microseparators [20–22]. Rebrov et al. [23] employed a ZSM-5 coated microchannel reactor for catalytic reduction of NO with ammonia. They reported that the better mass transport rate in the microchannel is responsible for the excellent conversion rate. Wan et al. [20] conducted 1-pentene epoxidation in a titanium silicalite-1 (TS-1) coated T-microchannel reactor. Higher 1,2-epoxypentane product yield was obtained with narrower channel width.

Separation processes can benefit directly from the large surface area-to-volume ratio that can be obtained in a microseparator. In fact, a few separation processes, such as extraction and membrane separation have been successfully miniaturized. There is a growing interest in the application of miniature transport membranes in sensors, microseparators and microreactors, as well as component parts of a lab-on-a-chip microdevices. Most of the research on micromembranes focuses on palladium [24–27] and polymer materials [28,29]. Hydrogen separation and purification from both gas and reaction mixtures were successfully conducted in palladium micromembranes [24–26]. Schiewe and coworkers [28] employed a polymeric membrane in a microreactor to enrich the ethylene oxide product from ethylene epoxidation. Martin et al. [29] used a porous polyimide membrane in a microchannel liquid–liquid contactor to transport dissolved 1-hexanol between hexane and water solvents. Mesoporous alumina and silica membranes made by anodization were also used as membrane contactor in miniature separation devices [30]. More recently, we have successfully made zeolite micromembranes and tested their permeation properties for different gases and hydrocarbon vapors [18,19,22]. Excellent permselectivity was obtained using the zeolitic membranes.

## 2. Experimental

### 2.1. Membrane microreactor design and fabrication

The microreactor unit consisted of a multi-channel plate and a stainless steel housing (Fig. 1a). The multi-channel plate was made by cutting microchannels onto the 25 mm × 25 mm metal plate using electro-discharge micromachining (AGIE Wirecut 120). The porous stainless steel (SS-316L) plates with a nominal pore size of 0.2 μm were purchased from Mott metallurgical corporation. Thirty-five microchannels, each 300 μm wide, 600

μm deep and 25 mm long, were cut onto the stainless steel plate. The multi-channel plate was cleaned with detergent and water to remove dirt and contaminants. The stainless steel plate was sonified in dilute nitric acid solution (69%, BDH) to remove oxide layers, followed by ethanol and acetone rinses before drying in an oven at 348 K.

The stainless steel housing (Fig. 1b and c) was designed for rapid testing of prototype microsystem architecture and to serve as an interface between the microsystem and macro-scale laboratory environment. The housing was machined from a single block of stainless steel (SS-316) plate

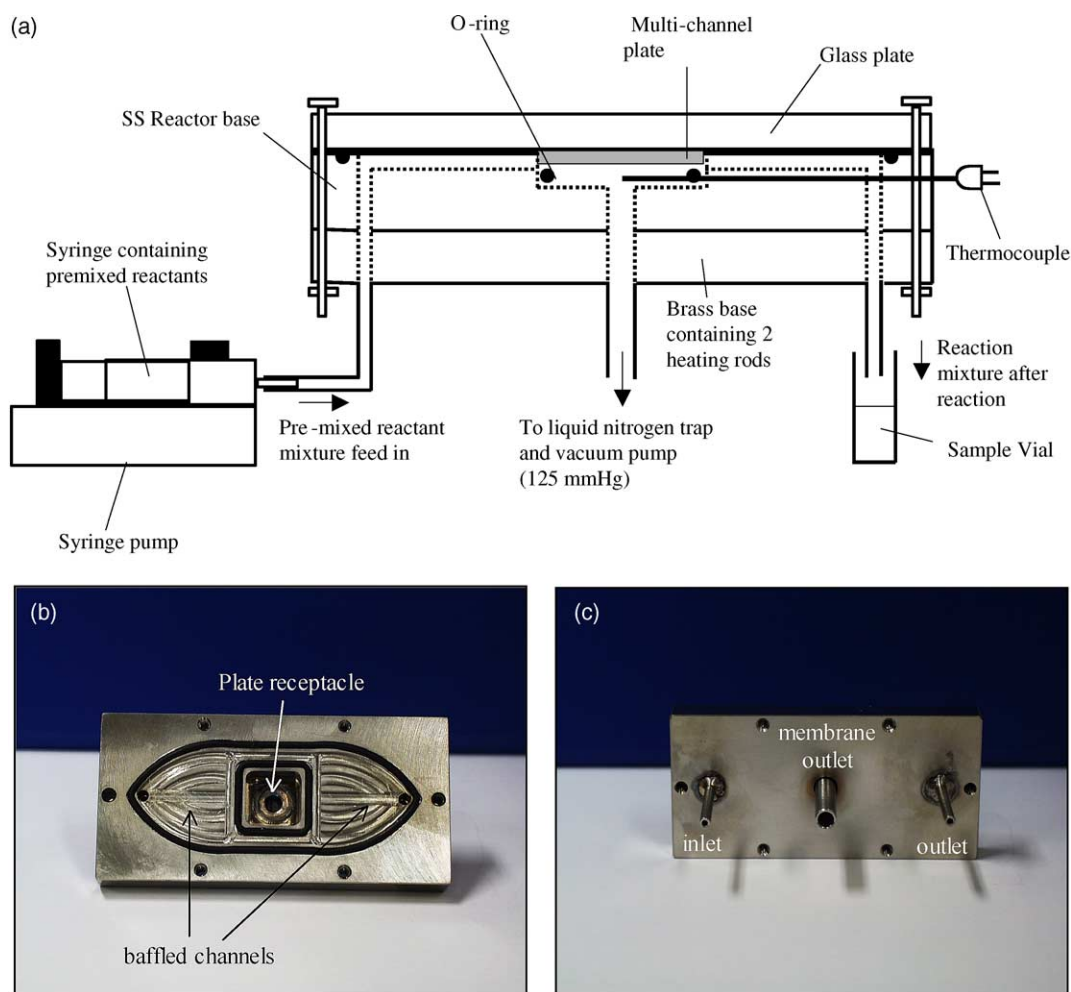


Fig. 1. (a) A schematic diagram of the microreactor set-up used in the Knoevenagel condensation reaction of benzaldehyde and ethyl cyanoacetate. (b) Top and (c) bottom pictures of the stainless steel housing.

and consisted of a receptacle for the multi-channel plate, inlet and outlet ports for the reaction fluid, and feedthroughs for sensors and vacuum (Fig. 1b). The fluid ports and feedthroughs are located beneath the housing unit as shown in Fig. 1c. Liquid reactants fed by a syringe pump (Kd Scientific) entered the inlet port into a narrow rectangular channel (1 mm × 25 mm) formed between the housing and the Pyrex glass cover. The liquid was evenly distributed along the width of the channel by a set of baffles before it reached the multi-channel plate (cf. Fig. 1b). This ensured that the liquid flowed uniformly through each of the microchannels. A similar set of baffles channeled the liquid leaving the multi-channel plate to the exit port, where it was collected in a sealed vial kept at room temperature for later analysis. Located beneath the receptacle holding the multi-channel plate was the vacuum port (cf. Fig. 1c) connected to a pressure gauge and a vacuum pump (Barnant Company). A liquid nitrogen trap was used to condense and collect the vapor that per-vaporated across the zeolite membrane. Thermocouples were inserted at different locations to measure the temperature of the entering and exiting fluid and that of the multi-channel plate. Heat was provided by a brass, heating block equipped with a pair of heating rods controlled by a temperature controller (Rex-C100, RKC).

## 2.2. Catalyst preparation, characterization and testing

Cs-exchanged NaX catalyst for Knoevenagel condensation reaction was prepared from NaX powder (Molecular Sieve 13X, Aldrich). The zeolite powder, 20 g (calcined in air at 673 K for 6 h to remove adsorbed contaminants) was added to 200 ml of 0.5 M cesium chloride (>98%, Sigma). The ion exchange was conducted at 353 K for 6 h. The powder was filtered, washed with warm distilled, deionized water and dried overnight in an oven at 338 K. The ion exchange was repeated for two more times before the powder was calcined in air for 4 h at 673 K. The catalyst was then crushed and sieved to produce a fine powder and examined by X-ray diffraction (XRD, Philips 1830), scanning electron microscopy (SEM, JEOL 6300 and

Philips XL30), nitrogen physisorption (Coulter SA3100), X-ray fluorescence spectroscopy (XRF, JEOL JSX-3201Z) and X-ray photoelectron spectroscopy (XPS, Physical Electronics PHI 5600) to determine its microstructure and composition.

The catalyst activity was tested in a common 3-necked glass batch reactor (10 ml). Equimolar amounts of benzaldehyde (99%, RDH) and ethyl cyanoacetate (98+%, Aldrich) were used in the experiment with 2 wt.% loading of catalyst. The reaction was conducted under well-mixed condition in a nitrogen atmosphere at 363, 393 and 413 K using 0.24 moles of each reactant. At fixed time intervals, reaction samples were withdrawn using a syringe, which were quenched with ice and centrifuged to remove the catalyst powder. Ten microliters of the reaction solution was diluted with 1 ml of tert-butyl methyl ether (MTBE, 99.8%, Fluka) and injected in a gas chromatograph (GC, HP 5890) equipped with a HP-5 column (30 m, HP) and a flame ionization detector. Three GC measurements were made for each sample and the concentration of the reactants and products were determined using a calibration curve prepared from standard solutions containing known quantities of benzaldehyde, ethyl cyanoacetate and ethyl 2-cyano-3-phenylacrylate (98%, TCI).

Cs-exchanged NaX catalyst was deposited onto the microchannels by the following procedure. A thin layer of polydiallyldimethylammonium chloride (PDAMAC, MW = 200,000–350,000, Aldrich) was coated onto the microchannel from a 20 wt.% PDAMAC solution. The coating was applied using a brush and was blown dried with compressed air. The multi-channel plate was pressed face down against a clean glass plate. Two milliliters of dilute catalyst suspension (1 wt.%) in water was placed near the channel openings and drawn into the microchannel with the aid of a light suction. The negatively charged zeolite particles were deposited onto the positively charged PDAMAC-coated microchannel walls. After drying at room temperature, the plate was calcined at 623 K for 4 h to burn away the PDAMAC organic coating and to partially sinter the coated zeolite onto the metal plate. The amount of deposited catalyst was determined from the weight difference between the coated and uncoated multi-channel plate. Visual inspection

using optical microscope and detailed imaging by SEM provided information on the catalyst coverage within the microchannels.

### 2.3. Membrane synthesis and characterization

Hydrophilic ZSM-5 zeolite membrane was grown on the backside of the multi-channel plate by ex situ synthesis method [31] involving pre-seeding and zeolite regrowth. The plate was brushed with 0.05 M mercapto-3-propyltrimethoxysilane (95%, Aldrich) in ethanol solution followed by a coating of TPA-silicalite-1 zeolite seeds (100 nm) from a 1 wt.% seed-ethanol suspension. This procedure was repeated four times to obtain a uniformly seeded plate. The zeolite membrane was grown from a synthesis solution containing a molar composition of 80 tetraethyl orthosilicate (TEOS): 8 Al(OH)<sub>3</sub>:10 NaOH:1 tetrapropylammonium hydroxide (TPAOH): 20,000 H<sub>2</sub>O. Aluminum hydroxide was obtained by dissolving aluminum sulfate (98+%, Aldrich) in ammonium hydroxide (28–30%, Fisher Scientific) under a mild temperature (343 K). The resulting white precipitates were filtered and washed to obtain a wet aluminum hydroxide powder that was then dissolved in an aqueous solution containing 0.04 M sodium hydroxide (99%, Aldrich) and 0.014 M TPAOH (1.0 M, Aldrich). Constant stirring and occasional heating were needed to ensure a clear solution. 3.20 ml of TEOS (98%, Aldrich) was slowly added to the solution and the resulting mixture was stirred overnight to obtain a clear, homogeneous solution.

The multi-channel plate was placed horizontally on a Teflon sample holder with its seeded surface facing downward and the patterned surface fully wrapped with Teflon tape to prevent deposition. The plate and sample holder were placed in a Teflon container and 70 ml of synthesis solution was added until the plate was completely immersed. The Teflon container was sealed within a stainless steel autoclave vessel and placed in a 453 K oven for hydrothermal synthesis. The reaction was quenched rapidly to room temperature after 48 h of synthesis. The plate was rinsed with DDI water and dried, prior to inspection with an optical microscope and weighing to determine the amount and coverage of zeolite deposit. The synthesis procedure was re-

peated three times to grow a 30 μm thick ZSM-5 membrane. The final membrane was examined with XRD, SEM (JEOL 6300) and XPS to determine the membrane structure and composition.

After removing the organic template molecules (i.e., TPA<sup>+</sup>) trapped within the zeolite pores at 823 K, the ZSM-5 membrane was tested for pervaporation of water/benzaldehyde mixtures in the stainless steel housing shown in Fig. 1. The liquid solution was fed at a flow rate of 1 ml/h and the membrane pervaporation was conducted at a temperature of 373 K and vacuum pressure of 125 Torr. The retentate was cooled at room temperature and collected in a sample vial, whereas the permeate stream was condensed and collected in a liquid nitrogen trap. The liquids collected from the retentate and permeate were first weighed, before analysis by gas chromatography. The permeate flux ( $P$ ) in kg h<sup>-1</sup> m<sup>-2</sup> was calculated from:

$$P = \frac{P_M}{A} \quad (1)$$

where  $P_M$  is the average mass flow rate across the membrane in kg h<sup>-1</sup> and  $A$  is the membrane area in m<sup>2</sup>. The selectivity of the membrane separation ( $\alpha$ ) was calculated from the composition of the liquids collected from the retentate and permeate.

$$\alpha = \frac{(Y_{H_2O}/Y_{organics})}{(X_{H_2O}/X_{organics})} \quad (2)$$

where  $Y_i$  and  $X_i$  are weight fraction of component  $i$  in the permeate and retentate, respectively.

### 2.4. Microreactor performance study

Equimolar amounts of benzaldehyde and ethyl cyanoacetate were mixed in a nitrogen hood to prevent the formation of benzoic acid. A 25 ml syringe (Hamilton) was rinsed and filled with the reactant solution. Gas and vapor bubbles were removed by gently tapping the syringe. The pre-heated reactor (i.e., 373 K) was manually filled with the reactant solution, taking care that no bubbles were formed during the process. Once the reactor was filled, the syringe was transferred to the syringe pump and the liquid was fed at a fixed rate (i.e., 0.2–12 ml/h). Samples were collected only after two hours of reaction. Two sets of experiments

were conducted each day. At the start of the experiment, the multi-channel plate was ran as a microreactor with the permeate vacuum closed and the reaction solution was collected from reactor outlet at fixed intervals to determine the steady-state condition. In the second experiment, the vacuum was turned on and the multi-channel plate was operated as a membrane microreactor. Samples were obtained from both reactor and permeate outlets. The multi-channel plate was cleaned with ethanol at the end of the experiments.

Experiments indicated that solutions analyzed immediately after sampling from the reactor and solutions that were analyzed after being refrigerated (269 K) overnight gave the same composition. This means that the reaction solution could be quenched and stored for later analysis. Ten microliters of the reaction solution was diluted with 1 ml of tert-butyl methyl ether (MTBE, 99.8%, Fluka) and analyzed by gas chromatography. Three GC measurements were made for each sample and the concentration of the reactants and products were determined using the calibration curve. Samples collected from the permeate outlet was also analyzed by TOC analyzer (TOC 500, Shimadzu) after dilution with

DDI water to determine the amount of organic carbon. The benzaldehyde conversion and ethyl 2-cyano-3-phenylacrylate yield along with the permeate flux ( $P$ ) and membrane separation ( $\alpha$ ) were used to evaluate the microreactor and membrane microreactor performance.

Performance comparison was made with a laboratory-scale reactor shown in Fig. 2 and described in Table 1. The tube-and-shell reactor consisted of a ceramic tube and a stainless steel housing. The porous  $\alpha$ -alumina tube serves as a support for a 30  $\mu\text{m}$  thick ZSM-5 membrane. The membrane tube had an ID of 6.5 mm and a length of 75 mm providing a membrane area of 15.4  $\text{cm}^2$  and a reactor volume of 1.9  $\text{cm}^3$ . 3.6 g of Cs–NaX beads ( $\sim 2$  mm) were packed inside the ceramic tube to give a comparable catalyst loading per reactor volume as that of the microreactors. A syringe pump was used to deliver pre-mixed reactant solution at 2–17 ml/h to the preheated reactor unit. Since the zeolite membrane was impermeable to the organic reactants and products at the reaction temperature of 373 K, a packed bed reactor (PBR) can be simulated by running the reaction with the permeate vacuum closed. A packed bed

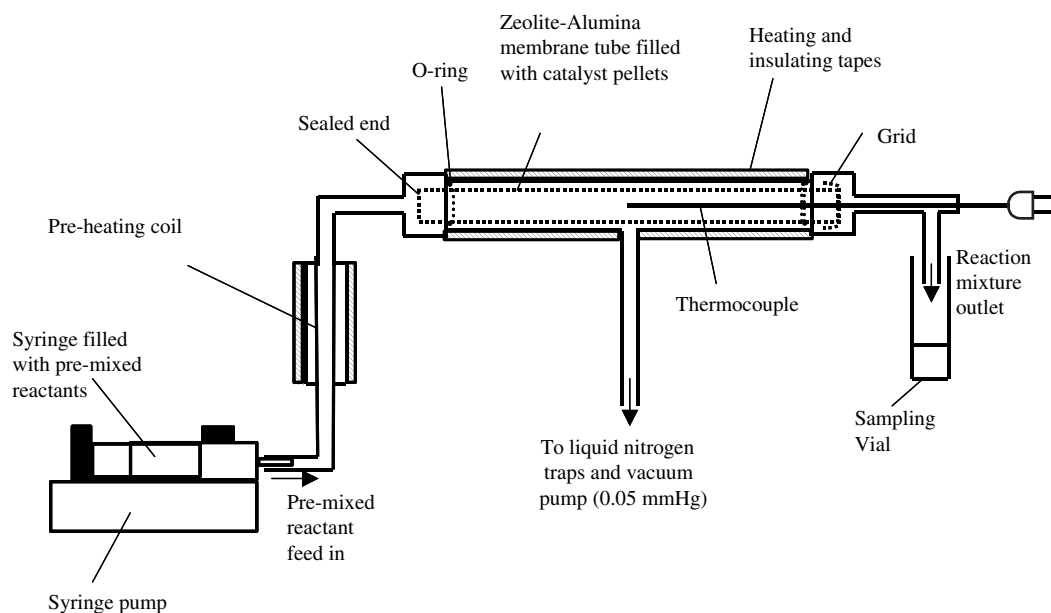


Fig. 2. Schematic diagrams of the tube-and-shell reactor for packed bed reactor (PBR) and packed bed membrane reactor (PBMR) experiments.

Table 1  
Reactor and catalyst descriptions

| Reactor   | Reactor size & geometry   | Flow rate                 | Catalyst                                     | Water removal  |
|---|---|---------------------------|--|--|
| Batch reactor                                     | Vol.: 10 cm <sup>3</sup>  | –                         | 0.03 g of 4 μm powder                        | Nil. <sup>a</sup>                                    |
| Packed bed reactor (PBR)                          | Cylindrical tube<br>ID: 0.65 cm<br>Length: 7.5 cm<br>Vol.: 1.9 cm <sup>3</sup>                | 2–17 cm <sup>3</sup> /h   | 3.6 g of 2 mm<br>Cs-exchanged<br>NaX beads   | Nil.   |
| Packed bed membrane reactor (PBMR) <sup>b</sup>   | Cylindrical tube<br>ID: 0.65 cm<br>Length: 7.5 cm<br>Vol.: 1.9 cm <sup>3</sup>                | 2–17 cm <sup>3</sup> /h   | 3.6 g of 2 mm<br>Cs-exchanged<br>NaX beads   | 4–20 g <sup>1</sup> m <sup>-2</sup> h <sup>-1</sup>  |
| Multi-channel microreactor                        | 35 channels<br>Width: 300 μm<br>Depth: 600 μm<br>Length: 2.5 cm<br>Vol.: 0.16 cm <sup>3</sup> | 0.2–12 cm <sup>3</sup> /h | 0.02 g of 4 μm<br>Cs-exchanged<br>NaX powder | Nil.   |
| Multi-channel, membrane microreactor <sup>c</sup> | 35 channels<br>Width: 300 μm<br>Depth: 600 μm<br>Length: 2.5 cm<br>Vol.: 0.16 cm <sup>3</sup> | 0.2–12 cm <sup>3</sup> /h | 0.02 g of 4 μm<br>Cs-exchanged<br>NaX powder | 20–80 g <sup>1</sup> m <sup>-2</sup> h <sup>-1</sup> |

<sup>a</sup> The bubble point temperature of the equimolar reactant mixture is 433 K and the final reaction mixtures obtained after 3 h of reaction at 363, 393 and 413 K have bubble point temperatures of 410, 403 and 390 K, respectively.

<sup>b</sup> 28-μm thick ZSM-5 (Si/Al = 35) membrane with a membrane area of 15.4 cm<sup>2</sup>.

<sup>c</sup> 30-μm thick ZSM-5 (Si/Al = 30) membrane with a membrane area of 6.25 cm<sup>2</sup>.

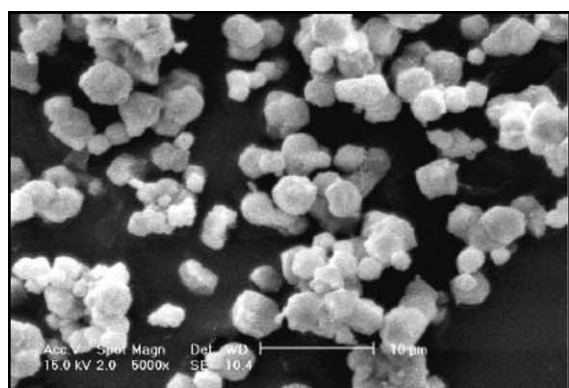
membrane reactor (PBMR) operation was obtained by simply turning the vacuum on. A vacuum pressure of 0.05 Torrs was generated using a rotary vacuum pump (Edwards Company). Reaction and permeate samples were collected by liquid nitrogen traps after steady-state reaction condition was reached. The samples were weighed and analyzed by gas chromatography to determine the reaction conversion and product yield.

### 3. Results and discussion

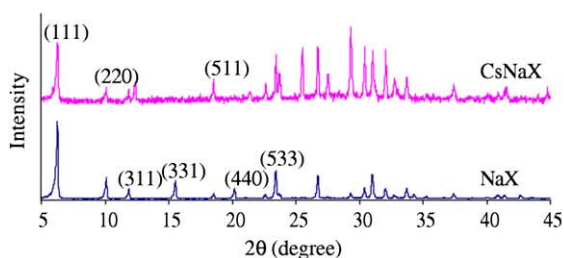
#### 3.1. Cs-exchanged NaX catalyst

Cs-exchanged NaX catalyst appears as agglomerated zeolite crystals in the SEM image of Fig. 3a. The catalyst displays similar morphology

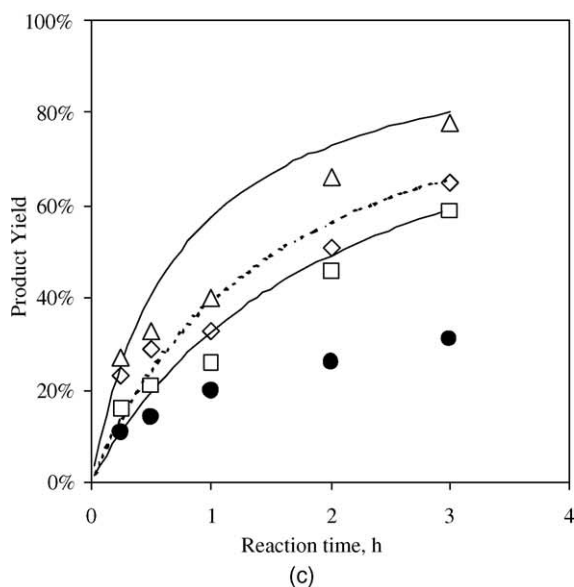
as the starting NaX zeolite. It can be seen in the figure that the individual zeolite crystals are roughly spherical in shape with poorly formed facets and have an average particle size of about 4 μm. Fig. 3b displays the X-ray diffraction patterns of the original NaX zeolite and the Cs-exchanged NaX catalyst. The calcined NaX powder displays the characteristic diffraction pattern of dehydrated NaX zeolite [32]. Ion exchange with CsCl led to weaker peak intensities and disappearance of the (3 3 1) and (4 4 0) diffraction lines. The presence of new diffraction peaks at  $2\theta = 12, 25.5, \text{ and } 27.5$  that had been assigned to Cs-exchanged NaX [33] indicated a successful catalyst preparation. A slight decrease in the surface area (i.e., 430–400 m<sup>2</sup>/g) was observed after cesium ion exchange. Rodriguez et al. [34] and Lasperas et al. [35] also made a similar observation. They reported that the



(a)



(b)



(c)

Fig. 3. (a) Scanning electron microscope picture of the Cs-exchanged NaX catalyst, (b) X-ray diffraction pattern of NaX and Cs-exchanged NaX powders, (c) Batch reaction data for Cs-exchanged NaX ( $\square$ , 363 K;  $\diamond$ , 393 K;  $\triangle$ , 413 K) and NaX catalysts ( $\bullet$ , 363 K). (Note: symbol, experimental data; line, model calculation).

decrease in catalyst surface area is directly proportional to the amount of ion exchanged cesium. It was suggested that the loss of surface area was caused by breakage of Si–O–Si bonds leading to pore collapse [36]. However, it is also possible that the smaller surface area was due to the restricted access to the zeolite pore channel caused by the presence of large cesium counterions [37]. Elemental analyses of the zeolite samples were performed by X-ray fluorescence spectroscopy (XRF) and X-ray photoelectron spectroscopy. The degree of ion exchange as measured by the Cs/(Na+Cs) ratio was about 0.78.

Fig. 3c displays the plots of benzaldehyde conversion as a function of reaction time for a batch reactor. The experiments were conducted at reaction temperatures of 363, 393 and 413 K for 180 min. Corma et al. [10] showed that interparticle diffusion resistance is negligible when the particle size of CsY catalyst is smaller than 250  $\mu\text{m}$  and the reaction was conducted under well-mixed conditions. Since zeolite X and Y belong to the same Faujasite family and possess similar pore structure, it is assumed that interparticle diffusion resistance is also negligible in the current catalyst. It can be seen from the figure that the activity of Cs-exchanged NaX catalyst is significantly higher than that of the precursor NaX zeolite. The Knoevenagel condensation reaction is an equilibrium-limited reaction [9] where benzaldehyde reacts with ethyl cyanoacetate to produce ethyl 2-cyano-3-phenylacrylate and water. Occasionally, benzoic acid is formed from poorly degassed mixtures, along with Michael addition byproducts [34]. Water produced by the reaction can adsorb in the zeolite and possibly poison the catalyst. Fig. 3c shows that the experimental data fit a reversible, second-order reaction kinetic equation. The calculated activation energy for the endothermic reaction is 18.3  $\text{kJ mol}^{-1}$ . This is lower than the values of 34–41  $\text{kJ mol}^{-1}$  reported by Corma et al. [10] for alkali metal cation zeolite X catalysts.

### 3.2. Multi-channel plate

Miniature devices including microelectromechanical systems (MEMS), chemical microsystems and bio-MEMS are mostly made of silicon mate-

rial. This is because of the well-established silicon microfabrication technology. However, silicon is rarely used in chemical production and material compatibility is an issue. Also, it is expensive compared to the traditional stainless steel used in reactor construction. New fabrication methods such as LIGA, excimer laser micromachining, electrochemical micromachining, ultrasonic micromachining, micro-spark erosion and micromilling were developed to enable the micromachining of a broader range of materials [7,38,39]. The excellent thermal and mechanical properties of stainless steel as well as its corrosion resistance make it a good candidate material for the construction of a microreactor. Indeed, Matson and coworkers [40] built a miniature fuel combustor for hydrogen production using stainless steel.

Conventional machining methods can produce channels as narrow as 200  $\mu\text{m}$ , but in order to prevent pore collapse in the porous stainless steel, electro-discharge micromachining (EDM) was used. This method can create microchannels as narrow as 100  $\mu\text{m}$  and as long as 100 mm with an aspect ratio as large as 10. Fig. 4a displays a picture of a multi-channel plate made from porous stainless steel by electro-discharge micromachining. Thirty-five microchannels, each 300  $\mu\text{m}$  wide, 600  $\mu\text{m}$  deep and 25 mm long, were machined onto the porous stainless steel plate. Unlike the plates made by conventional machining, the wall of the microchannels made by EDM remains porous and permeable to liquids and gases. The evenly spaced microchannels are clearly seen from the higher magnification SEM picture of Fig. 4b. The size and shape of the microchannel (Fig. 4c) correspond to the diameter and shape of the wire used to cut the channels. Each microchannel has a volume of 4.5  $\mu\text{l}$  giving the entire plate a reactor volume of 0.16 ml.

### 3.3. ZSM-5 membrane

Fig. 5a and b display the SEM pictures of ZSM-5 membranes grown on the multi-channel plate and on porous  $\alpha\text{-Al}_2\text{O}_3$  tube, respectively. Both stainless steel and aluminum oxide supports have the same nominal pore size of 0.2  $\mu\text{m}$ , but the porous stainless steel has a rougher surface and

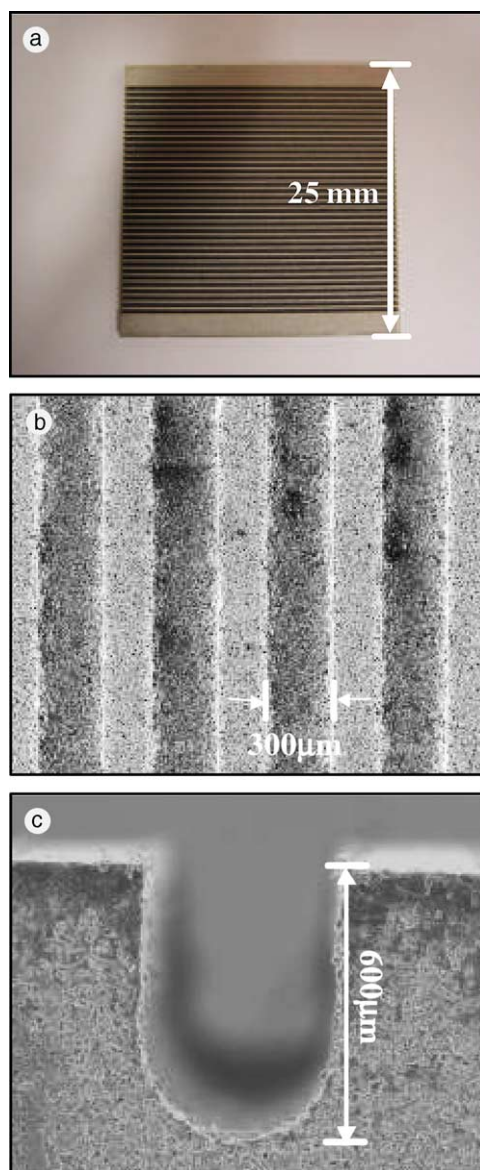


Fig. 4. (a) Optical and (b) scanning electron microscope pictures of the multi-channel plate with (c) a high magnification picture of the channel cross-section.

broader pore size distribution. Pores as large as ten microns were not unusual for the porous stainless steel and a minimum zeolite thickness of 25  $\mu\text{m}$  was needed to ensure a defect free membrane. This is the main reason for using a thick membrane layer, and for comparison purposes the same thickness was used for the membrane grown on

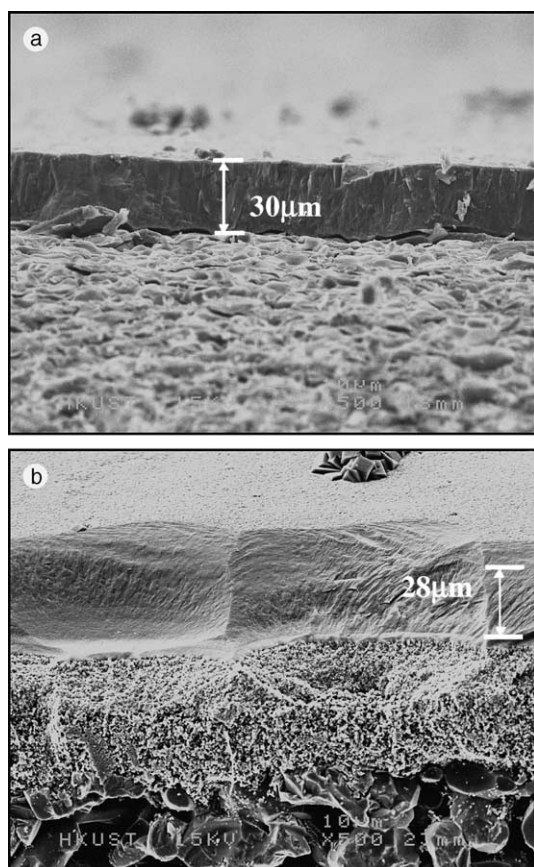


Fig. 5. Scanning electron micrographs of ZSM-5 membrane cross-section grown on (a) multi-channel plate and (b) porous alumina tube.

alumina support. The 30- $\mu\text{m}$  thick, ZSM-5 zeolite membrane (i.e., 25 mm $\times$ 25 mm) grown on the backside of the porous multi-channel plate is shown in Fig. 5a. X-ray diffraction analysis indicated that the well-intergrown membrane has a (002) film orientation. The membrane consisted of interlocked 20- $\mu\text{m}$  sized crystal grains. Test showed that prior to the removal of the organic template molecules (i.e., TPA<sup>+</sup>) trapped within the zeolite pores, the membrane is impermeable to gases. Elemental analysis showed that the membrane has a Si/Al ratio of 30. A slightly thinner, 28  $\mu\text{m}$  ZSM-5 membrane was grown on the  $\alpha$ -Al<sub>2</sub>O<sub>3</sub> tube (Fig. 5b). Analysis showed that the membrane has a similar microstructure and a comparable Si/Al ratio of 35.

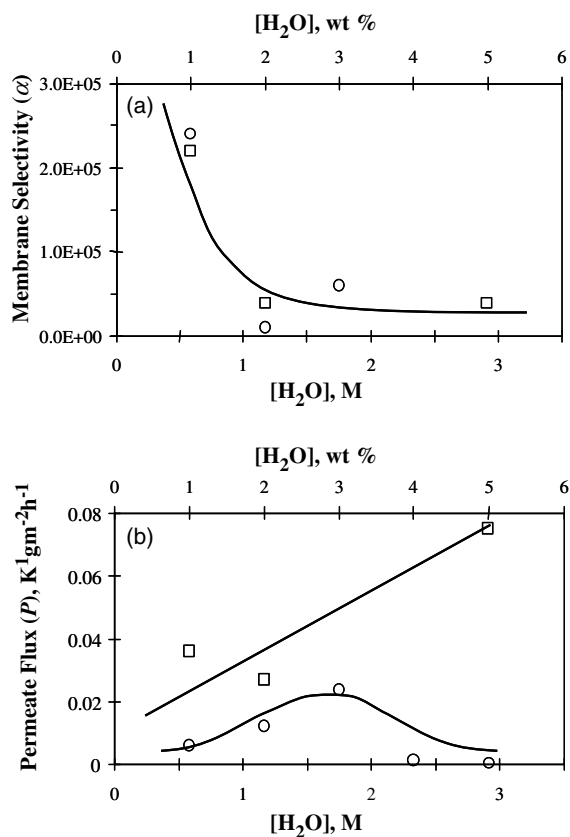


Fig. 6. Plots of the (a) membrane selectivity ( $\alpha$ ) and (b) permeate flux ( $P$ ) for water–benzaldehyde separation. ( $\square$ , multi-channel ZSM-5 membrane plate;  $\circ$ , ZSM-5/ $\alpha$ -Al<sub>2</sub>O<sub>3</sub> membrane tube.)

Fig. 6 plots the membrane selectivity ( $\alpha$ ) and permeate flux ( $P$ ) as a function of water concentration in a benzaldehyde solution. Both membranes exhibit very high selectivity for water as shown in Fig. 6a. A separation ratio of 240,000 was obtained at 1 wt.% water. This ratio decreased to about 50,000 for higher water concentrations. The hydrophilic nature of the ZSM-5 membrane, as well as its molecular-sized pores (i.e., 5.5 Å) are responsible for the excellent separation. The size of the benzaldehyde molecule is large and it diffuses through the membrane only with difficulty. Experiments showed that the ZSM-5 membrane was impermeable to pure benzaldehyde at temperatures below 423 K. Fig. 6b shows that the permeate flux through the multi-channel membrane

plate is larger than that of the tubular zeolite membrane even though the latter was operated under a higher vacuum (i.e., 0.05 vs. 125 Torr). This can be explained by the improved transport rate in a microsystem. Rapid mass and heat transfer rates are obtained in microchannel even under laminar flow regime because of the large interfacial surface area and short diffusion distance [4]. As expected, the permeate flux for the membrane micro-channel plate increases linearly with water concentration in the benzaldehyde solution.

The permeate flux of the tubular membrane behaves differently as shown in Fig. 6b. At low concentration, the permeate flux increases with water concentration reaching a maximum value of  $0.025 \text{ kg m}^{-2} \text{ h}^{-1}$  at about 3 wt.% water, but decreases rapidly at higher water concentrations. The poor solubility of water in benzaldehyde ( $\sim 0.6$  wt.% at 373 K) means that at high water concentration, the mixture is unstable and phase separation can occur resulting in the poor separation. Fig. 6b clearly shows that phase separation is not a problem for the multi-channel membrane plate. This suggests that either phase separation was suppressed in the microchannel or its effects were compensated by the enhanced mass transfer in the microchannel. Experimental evidence suggests that the latter is the more plausible explanation.

### 3.4. Microreactor and membrane microreactor performance

An estimated 0.02 g of Cs-exchanged NaX catalyst powder was uniformly coated onto the multi-channel membrane plate and was activated by pretreatment in air at 623 K for 4 h. A picture of the catalyst-coated microchannel is shown in Fig. 7a. The catalyst particles were trapped in the grooves and crevices of the porous stainless steel. A dry run was conducted to test the adhesion of the catalyst particles on the microchannels. Water–benzaldehyde solutions were flowed through the microchannels at 1 ml/h and 373 K for 20 h. Analysis of the reactor effluent at fixed intervals was unable to detect any dislodged particles. This clearly shows that there was a good catalyst adhesion on the microchannel. Parallel pervaporation experiments were conducted to determine the

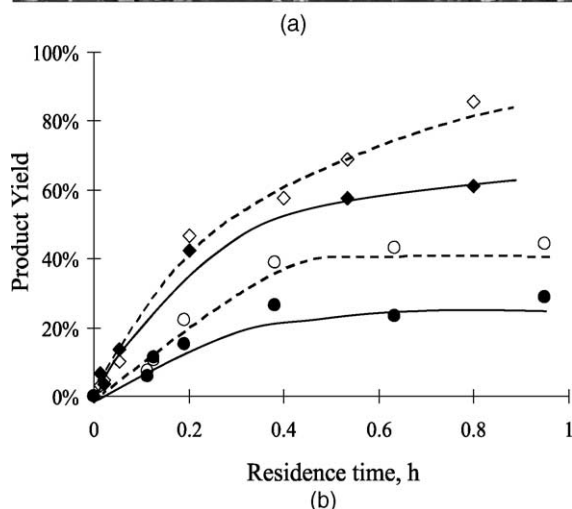
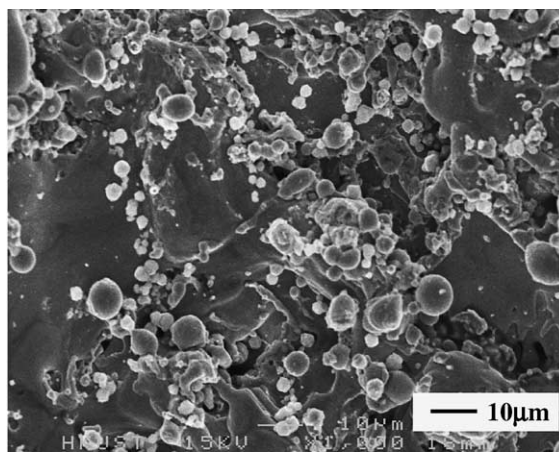


Fig. 7. (a) SEM picture of the Cs-exchanged NaX catalyst-coated microchannel. (b) Performance comparison between PBR (●), PBMR (○), microreactor (◆) and membrane microreactor (◇) for the Knoevenagel condensation reaction of benzaldehyde and ethyl cyanoacetate at 373 K.

effects of catalyst incorporation and pretreatment on the membrane. Experiments showed that the membrane separation and permeate flux remained unchanged after the addition of catalyst.

Preliminary reaction studies were conducted using a stoichiometric mixture of benzaldehyde and ethyl cyanoacetate on the porous stainless steel substrate and ZSM-5 zeolite membrane. The reaction temperature was set at 373 K and the flow rate at 1 ml/h. No ethyl 2-cyano-3-phenylacrylate was produced in these experiments and only a trace amount of benzoic acid was detected. This

indicates that both stainless steel and zeolite materials were inert under the reaction conditions. Catalyst activation and deactivation can occur during the normal course of a reaction, but can be easily remedied by stabilizing the catalyst under the reaction conditions. The stabilized, catalyst-coated multi-channel membrane plate (cf. Fig. 7a) was monitored for 70 h under reaction condition. Except for an initial 3% lost in activity, both benzaldehyde conversion (20%) and ethyl 2-cyano-3-phenylacrylate yield (19.8%) were constant throughout the experiment. It is important to note that in order to establish the steady-state condition, effluent and permeate samples were collected at discrete intervals for analysis. Three measurements were made from each sample and the results were averaged. Material and carbon balances showed that the outlet streams added up to within 95% of the inlet value.

Fig. 7b plots the product yield as a function of residence time for the packed-bed reactor (PBR), packed-bed membrane reactor (PBMR), microreactor and membrane microreactor. The residence time was calculated from the ratio of the reactor volume to the fed flow rate ( $\tau = V/F$ ). It is clear from the results that the performance of the packed-bed reactor is poor when compared to the other reactor systems. The highest yield obtained from the packed bed reactor is about 30%, whereas the microreactor reaches the maximum yield expected at equilibrium of 60%. This equilibrium value was estimated by running the batch reaction for a longer time (i.e., 12 h) using a higher catalyst loading (i.e., 20 wt.%). The poor performance of the PBR is due to the large external mass transfer resistance along the catalyst bed, which is absent in the microreactor. Better mass transfer rate is one of the characteristic features of a microreactor, which also include high heat transfer rate and narrow residence time distribution. However, inter- and intra-particle diffusion resistances are independent of the reactor design and only depend on the catalyst. It is safe to assume that the interparticle diffusion resistance of the coated zeolite layer is insignificant when compared to the transport resistance through the zeolite pores. Intraparticle diffusion can be improved by using a zeolite catalyst with a smaller particle size (i.e.,  $<4 \mu\text{m}$ ).

Simply turning on the vacuum transformed the PBR into a packed-bed membrane reactor. An increase in conversion and product yield (i.e., up to 45%) was observed for the PBMR, but the values are significantly less than the expected equilibrium yield of 60% (Fig. 7b). TOC analysis of the samples from the membrane outlet indicated that pure water was pervaporated through the ZSM-5 membrane during the reaction. An average pervaporation rate of  $0.04 \text{ kg m}^{-2} \text{ h}^{-1}$  was obtained at a residence time of 0.13 h, which gradually increases to a value of  $0.15 \text{ kg m}^{-2} \text{ h}^{-1}$  at  $\tau = 0.8 \text{ h}$ . Although the selective removal of water by PBMR eliminated the thermodynamic constraint, the reaction still suffered from the same poor mass transport rate experienced by the PBR. This problem was solved using a membrane microreactor. A product yield of 85% was obtained from the membrane microreactor. Calculations indicated that all the water produced by the condensation reaction was completely removed by the membrane and the membrane is operating below its capacity. This suggests that the performance of the membrane microreactor is limited mainly by the kinetics, now that both thermodynamic and mass transfer constraints were removed.

#### 4. Concluding remarks

This work clearly demonstrated the potential application of membrane microreactor for clean and efficient synthesis of fine chemicals. The use of heterogeneous zeolite catalysts in the test reaction enabled us to avoid the use of hazardous, homogeneous catalyst and also eliminated the need for solvents. This significantly reduced waste generation and lowered the cost of downstream separation. The improved mass transport rate in the microchannel led to a higher per pass yield compared to the traditional packed bed reactors (e.g., PBR and PBMR). It was also responsible for the better membrane performance in microsystem. The selective removal of the byproduct from the reaction was shown to eliminate the thermodynamic constraint leading to supra-equilibrium conversion. It also improved the product purity

and prolonged the catalyst life by removing the water byproduct.

Although there are clear advantages in the use of microreactors (i.e., including membrane microreactors), further improvements in their design and fabrication are needed in order to reduce their cost and increase their productivity. Substitution of stainless steel for silicon is one step toward cost reduction, but this is currently offset by the cost of micromachining and fabrication. Alternative fabrication methods amenable for mass production such as casting or stamping must be developed. A new rationale for microsystem architecture must break away from the two-dimensional blueprint inherited from the microelectronic and MEMS fabrications. The new architecture must exploit the three-dimensional space to create a flexible and efficient microreactor design. Strategies for precise and selective incorporation of active elements such as catalyst, membrane, adsorbent, contactor and sensors must be established. In order to succeed against the batch reactor as a tool for discovery and production, the microreactor hardware development must be conducted in close partnership with synthetic chemists.

### Acknowledgements

The authors would like to thank the Institute for Integrated Microsystems (I2MS-01/02.EG02) for funding this research. We also would like to acknowledge the Microfabrication Facility (MFF) and Material Preparation and Characterization Facility (MCPF) of Hong Kong University of Science and Technology.

### References

- [1] K.F. Jensen, *AIChE J.* 45 (1999) 2051.
- [2] N. Kawahara, T. Suto, T. Hirano, Y. Ishikawa, T. Kitahara, N. Ooyama, T. Ataka, *Microsystem Technol.* 3 (1997) 37.
- [3] W. Ehrfeld, V. Hessel, S. Kiesewalter, H. Lowe, Th. Richter, J. Schiewe, *Microreaction technology: industrial prospects*, in: W. Ehrfeld (Ed.), *Proceedings of the Third International Conference on Microreaction Technology*, Springer, Berlin, 1999, p. 14.
- [4] J.R. Burns, C. Ramshaw, *Trans. I. Chem. Eng.* 77 (1999) 206.
- [5] W. Ehrfeld, V. Hessel, H. Löwe (Eds.), *Microreactors: New Technology for Modern Chemistry*, Wiley-VCH, Weinheim, 2000.
- [6] K.F. Jensen, *Chem. Eng. Sci.* 56 (2001) 293.
- [7] A. Gavriilidis, P. Angeli, E. Cao, K.K. Yeong, Y.S.S. Wan, *Trans. I. Chem. Eng.* 80 (2002) 3.
- [8] O. Wörz, K.P. Jäckel, Th. Richter, A. Wolf, *Chem. Eng. Sci.* 56 (2001) 1029.
- [9] L.F. Tietze, U. Beifuss, in: B.M. Trost, I. Fleming (Eds.), *Comprehensive organic synthesis: Selectivity, strategy and efficiency in modern organic chemistry*, Pergamon Press, England, 1991, p. 341.
- [10] A. Corma, V. Fornes, R.M. Martin-Aranda, H. Garcia, *J. Primo, Appl. Catal.* 59 (1990) 237.
- [11] A. Corma, R.M. Martin-Aranda, F. Sanchez, in: M. Guisnet, J. Barrault, C. Bouchoule, D. Duprez, R. Maurel, C. Montassier (Eds.), *Heterogeneous Catalysis and Fine Chemicals II, Studies in Surface Science and Catalysis*, vol. 62, Elsevier, Amsterdam, 1991, p. 503.
- [12] A. Corma, R.M. Martin-Aranda, *Appl. Catal. A* 105 (1993) 271.
- [13] I. Rodriguez, H. Cambon, D. Brunel, M. Lasperas, *J. Mol. Catal. A* 130 (1998) 195.
- [14] A. Corma, R.M. Martin-Aranda, F. Sanchez, *J. Catal.* 126 (1990) 192.
- [15] S. Ernst, T. Bongers, C. Casel, S. Munsch, in: I. Kiricsi, G. Pal-Borbely, J.B. Nagy, H.G. Karge (Eds.), *Porous Materials in Environmentally Friendly Processes, Studies in Surface Science and Catalysis*, vol. 125, Elsevier, Amsterdam, 1999, p. 367.
- [16] M. Lasperas, T. Llorett, L. Chaves, I. Rodriguez, A. Cauvel, D. Brunel, *Heterogeneous catalysis and fine chemicals IV*, in: H.U. Blaser, A. Baiker, R. Prins (Eds.), *Studies in Surface Science and Catalysis*, vol. 108, Elsevier, Amsterdam, 1997, p. 75.
- [17] J.G.S. Marcano, T.T. Tsotsis, *Catalytic Membranes and Membrane Reactors*, Wiley-VCH, Weinheim, 2002, p. 97.
- [18] Y.S.S. Wan, J.L.H. Chau, A. Gavriilidis, K.L. Yeung, *Microporous Mesoporous Mater.* 42 (2001) 157.
- [19] J.L.H. Chau, Y.S.S. Wan, A. Gavriilidis, K.L. Yeung, *Chem. Eng. J.* 88 (2002) 187.
- [20] Y.S.S. Wan, A. Gavriilidis, J.L.H. Chau, K.L. Yeung, *Chem. Commun.* 8 (2002) 878.
- [21] J.L.H. Chau, K.L. Yeung, *Chem. Commun.* 9 (2002) 960.
- [22] A.Y.L. Leung, J.L.H. Chau, K.L. Yeung, *Lab-on-a-Chip*, in press.
- [23] E.V. Rebrov, G.B.F. Seijger, H.P.A. Calis, M.H.J.M. de Croon, C.M. van den Bleek, J.C. Schouten, *Appl. Catal. A* 206 (2001) 125.
- [24] D.J. Quiram, I. Hsing, A.J. Franz, K.F. Jensen, M.A. Schmidt, *Chem. Eng. Sci.* 55 (2000) 3065.
- [25] S.V. Karnik, M.K. Hatalis, M.V. Kothare, *J. Microelectromech. Sys.* 12 (2003) 93.
- [26] K. Kusakabe, S. Morooka, H. Maeda, *Korean J. Chem. Eng.* 18 (2001) 271.

- [27] T. Cui, J. Fang, A. Zheng, F. Jones, A. Reppond, *Sens. Actuators, B* 71 (2000) 228.
- [28] B. Schiewe, C. Staudt-Bickel, A. Vuin, G. Wegner, *Chem. Phys. Chem.* 2 (2001) 211.
- [29] P.M. Martin, D.W. Matson, W.D. Bennett, *Chem. Eng. Commun.* 173 (1999) 245.
- [30] S. Haswell, V. Skelton, *Trac-Trend Anal. Chem.* 19 (2000) 389.
- [31] J.L.H. Chau, C. Tellez, K.L. Yeung, K. Ho, *J. Membr. Sci.* 164 (2000) 257.
- [32] M.M.J. Treacy, J.B. Higgins, R. Ballmoos, *Collection of Simulated XRD Powder Patterns for Zeolites*, Elsevier, New York, 1996, pp. 446–447 & 524–525.
- [33] C.E.A. Kirschhock, B. Hunger, J.A. Martens, P.A. Jacobs, *J. Phys. Chem. B* 104 (2000) 439.
- [34] I. Rodriguez, H. Cambon, D. Brunel, M. Lasperas, P. Geneste, in: M. Guisnet, J. Barbier, J. Barrault, C. Bouchoule, D. Duprez, C. Montassier, G. Perot (Eds.), *Heterogeneous Catalysis and Fine Chemicals III*, *Studies in Surface Science and Catalysis*, vol. 78, Elsevier, Amsterdam, 1993, p. 623.
- [35] M. Lasperas, H. Cambon, D. Brunel, I. Rodriguez, P. Geneste, *Microporous Materials* 7 (1996) 61.
- [36] K.R. Kloetstra, H. van Bekkum, in: H. Chon, S.-K. Ihm, Y.S. Uh (Eds.), *Progress in Zeolite and Microporous Materials, Studies in Surface Science and Catalysis*, vol. 105, Elsevier, Amsterdam, 1997, p. 431.
- [37] U. Ryma, M. Hunger, H. Knozinger, J. Weitkamp, in: I. Kiricsi, G. Pal-Borbely, J.B. Nagy, H.G. Karge (Eds.), *Porous Materials in Environmentally Friendly Processes, Studies in Surface Science and Catalysis*, vol. 125, Elsevier, Amsterdam, 1999, p. 197.
- [38] P.M. Martin, D.W. Matson, W.D. Bennett, *Chem. Eng. Commun.* 173 (1999) 245.
- [39] W. Ehrfeld, V. Hessel, J. Lehr, in: A. Manz, H. Becker (Eds.), *Top. Curr. Chem.*, vol. 194, Elsevier, Amsterdam, 1998, p. 369.
- [40] D.W. Matson, P.M. Martin, D.C. Stewart, A.L.Y. Tonkovich, M. White, J.L. Zilka, G.L. Roberts, *Microreaction technology: industrial prospects*, in: W. Ehrfeld (Ed.), *Proceedings of the Third International Conference on Microreaction Technology*, Springer, Berlin, 1999, p. 62.